Inorganic Chemistry

pubs.acs.org/IC

Communication

Rapid and Accurate Prediction of the Axial Magnetic Anisotropy in Cobalt(II) Complexes Using a Machine-Learning Approach

Henrique C. Silva Junior, Heloisa N. S. Menezes, Glaucio B. Ferreira,* and Guilherme P. Guedes*

Cite This: https://doi.org/10.1021/acs.inorgchem.3c02569

Read Online

ACCESS | Metrics & More | Article Recommendations | Supporting Information

ABSTRACT: Estimating the magnetic anisotropy for single-ion magnets is complex due to its multireference nature. This study demonstrates that deep neural networks (DNNs) can provide accurate axial magnetic anisotropy (D) values, closely matching the complete-active-space self-consistent-field (CASSCF) quality using density functional theory (DFT) data. We curated an 86-parameter database (UFF1) with electronic data from over 33000 cobalt(II) compounds. The DNN achieved an R^2 of 0.906 and a mean absolute error of 18.1 cm^{-1} in comparison to reference CASSCF D values. Remarkably, it is 11 times more accurate than DFT methods and 7700 times faster. This approach hints at DNNs predicting the anisotropy in larger molecules, even when trained on smaller ligands.

Single-molecule magnets (SMMs) are metal−organic compounds exhibiting magnetic hysteresis below a specific temperature without relying on intermolecular interactions. First reported in the 1990s as $[Mn_{12}O_{12}(CH_3COO)_{16}(H_2O)_4]$,[1,2] their potential applications include magnetic memory miniaturization[3] and, recently, spin qbits in quantum computing.[4] Initial misconceptions[5] about enhancing relaxation barriers through polynuclear SMMs were debunked. Instead, coordination compounds with a single metal center showed improved relaxation times, leading to the study of single-ion magnets (SIMs). While lanthanides received attention for their magnetic anisotropy,[6,7] their increase in anisotropy did not correlate with the magnetic bistability.[8] Transition metals, although having minor anisotropy compared to lanthanides, are advantageous because of their design flexibility for high energy barriers and magnetic bistabilities.[9−11] Among them, cobalt(II) stands out for its rich coordination chemistry[12,13] and varied magnetic anisotropy range.[14]

Studying the magnetic anisotropy merges experimental and computational methods. Computationally, despite advancements, the determination of magnetic anisotropy remains challenging. Density functional theory (DFT) often falters,[15,16] reinforcing Griffith's theory[17] that spin−orbit couplings greatly influence zero-field splitting (ZFS) on transition metals. Thus, chemists resort to intricate methods like complete-active-space self-consistent field (CASSCF) and multireference configuration interaction, which are computationally intensive.

The rapid advance of machine-learning (ML) techniques in the past few years has brought the promise of revolutionizing various aspects of human society because it has been demonstrated that any function can be approximated by a neural network (NN) with a sufficient number of neurons and adequate data.[18,19] Despite still being in its infancy, the fields of molecular and materials science are already benefiting from scientific ML in several applications, such as energetics[20,21] and molecular dynamics.[22] Although applications in the multiscale molecular magnetism field are still relatively scarce, recent works have begun developing prototypical procedures to address the complexities of the spin Hamiltonian,[23] spin dynamics,[24] and spin−phonon coupling over large clusters,[25] in addition to attempts to describe the dynamic $\mathbf{g}$ and anisotropic tensors in vibronically active systems.[26−28]

Because our group has gathered a significant amount of experience in molecular magnetism using DFT and multireference ab initio calculations, we decided to go beyond the traditional computational methods to evaluate whether a ML-oriented approach could be reliably used to obtain the axial magnetic anisotropy component (D) from the effective spin Hamiltonian (eq 1) by correlating single-reference DFT properties to multireferential CASSCF D values, reducing the difficulties of using multireferential methods.

$$\hat{H}_{ZFS} = D\left[\hat{S}_z^{\,2} - \frac{1}{3}S(S+1)\right] + E(\hat{S}_x^{\,2} - \hat{S}_y^{\,2}) \quad (1)$$

For the purposes of this work, we created a large DFT and CASSCF database containing the geometric and electronic properties of Co^{II} SIMs. To do so, we selected a bottom-up approach, starting from the more straightforward cases possible and building up to more complicated molecular configurations. Because our initial proof-of-concept is the cobalt(II) compounds, at this point, only 2+ oxidation states are considered. Simple Werner ligands, such as ammonia, and water were used to construct Co^{II} molecular models with coordination numbers ranging from 2 to 6 in all possible bonding combinations, accounting for a total of 32 unique

Received: July 26, 2023

initial structures (Figure S1). All calculations used the ORCA software.[29] Each structure was initially optimized on the PBEh-3c[30] composite scheme. Then, a rigid scan was performed on the TPSS/Def2-TZVP and CAS(7,5)/Def2-TZVP levels to extract electronic data, changing the Co−O bond from 1.7 to 2.8 Å and Co−N from 1.6 to 2.7 Å and allowing X−Co−Y bond angles to interconvert one valence shell electron pair repulsion configuration into another (i.e., seesaw to trigonal bipyramidal, linear to bent, etc.), as described in detail in the DFT and CASSCF Protocol section. The resulting database, which we call UFF1, contains 33731 data points with 86 parameters sectionalized between geometric, DFT, and CASSCF features (see List S1 for a full parameter list). Following an initial data engineering analysis for the ML training conducted in this study, all low-spin Co^{II} molecules (exactly 100) identified by state-averaged CASSCF (SA-CASSCF) were excluded from the training set.

As previously discussed, DFT usually provides D values that are considered mostly useless for transition-metal anisotropy[15,31,32] compared to the reference CASSCF values. A comparison of the D components calculated using DFT and CASSCF for a sample of 1100 geometric variations of the hexacoordinated $[Co(OH_2)_6]^{2+}$ compound shows that DFT largely underestimates the anisotropy, remaining within the −5 to +15 cm^{-1} range, while CASSCF predicts a −155 to +95 cm^{-1} range for the same sample, much more in accordance with that expected for the Co^{II} ion.[11] Indeed, D_{DFT} had such a poor performance [R^2 = −5.32 and mean absolute error (MAE) = 117.70 cm^{-1} in Figure S2] that we decided to drop these values from the UFF1 database.

The calculation of over 33000 D_{CASSCF} values in this work provided a comprehensive overview of Co^{II} anisotropy, establishing that the ion's maximum theoretical anisotropy range should lie between −255 and 167 cm^{-1} (Figure 1).

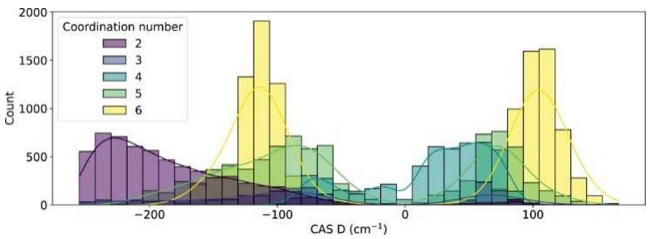

Figure 1. Histogram plots of 33631 cobalt(II) compounds separated by coordination numbers and CASSCF D values (cm^{-1}).

These values are corroborated by the literature, which confirms that the highest negative anisotropy for cobalt is achieved in compounds with low coordination numbers,[33] while high positive anisotropy[34] is typically found in compounds with high coordination numbers (Table S2).

To illustrate the intricate interplay between the anisotropy and geometric variations, we meticulously analyzed a data set comprised of 1961 CAS(7,5) D samples of the bicoordinate $[Co(NH_3)(OH_2)]^{2+}$, with bond lengths and angles spanning 1.8−2.7 Å and 75−180°, respectively (refer to the Supporting Information for further details). As depicted in Figure 2, the 3D plot of CASSCF axial anisotropy versus geometry underscores a complex correlation between these factors. This serves as a stark reminder of the difficulties encountered by predictive methods not grounded in ab initio principles.

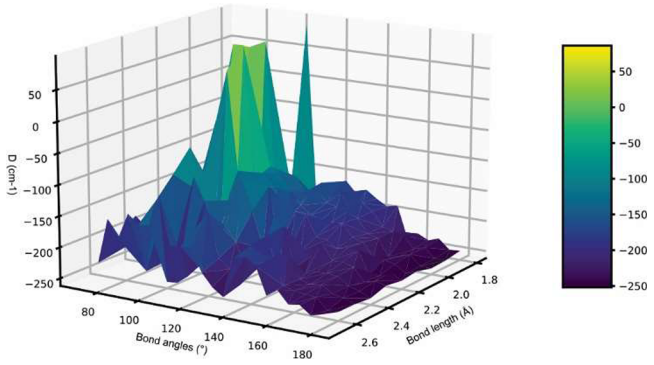

Figure 2. CAS(7,5) surface describing the variation in the anisotropy as the bond lengths and angles change on the two-coordinate model $[Co(NH_3)(OH_2)]^{2+}$.

Because magnetic anisotropy manifests itself on the metal ion due to effects on the ZFS and spin−orbit coupling, the ligands themselves are reduced to the role of "field generators";[35,36] consequently, our ML approach emphasizes the cobalt properties rather than explicitly incorporating the ligands' geometries into the training features, which is distinct from the approach used by recent works[26−28] aiming to predict **D** tensors using full geometric descriptions. The clear advantage of our approach is that, by excluding the explicit ligands' geometries (because their effects are implicitly added to the magnetic ion's response), our model is not size-restricted by representations such as Coulomb matrixes. After conducting several tests (refer to the Machine Learning Protocol section for detailed reasoning on our featured choice), we selected the most effective **training features** $X(f_{DFT})$ of coordination number, DFT spin deviation, DFT SOMO−LUMO gap, DFT SOMO-1−LUMO gap, DFT SOMO-2−LUMO gap, DFT dipole moment X, DFT dipole moment Y, and DFT dipole moment Z, and the **target/response** $y(f_{CAS})$ is CAS H_{eff} D, which contains D values obtained from the effective spin Hamiltonian calculated by SA-CASSCF. Our examination of the correlation matrix, comprising selected DFT features $X(f_{DFT})$ and CASSCF D response $y(f_{CAS})$ (Figure S3), reveals no direct, positive, or negative correlation. The data's inherent complexity, potentially high dimensionality, and nonlinear interplay of variables underscore the necessity of more refined ML techniques because basic data-fitting approaches prove insufficient.

The training was performed as indicated in Correlation 1, employing a feedforward dense neural network (DNN) on *TensorFlow*, version 2.12,[37] software running on the GPU-powered Google Colaboratory.[38] The architecture of the network was determined by a random search using Keras-tuner and uses an input layer with eight neurons, followed by five hidden layers containing 552, 424, 552, 424, and 72 neurons and an output layer with a single neuron. The setup used scaled exponential linear units[39] (SeLU) as the activation function (Function 2) and the Adamax[40] optimizer with the learning rate set to 0.0005. Our data were partitioned into 80% training, 10% testing, and 10% validation sets.

$$X(f_{DFT}) \rightarrow y(D_{CAS}) \qquad \text{(Correlation 1)}$$

$$f(x) = \begin{cases} \lambda x & \text{if } \geq 0 \\ \lambda\alpha(e^x - 1) & \text{if } x < 0 \end{cases} \qquad \text{(Function 2)}$$

https://doi.org/10.1021/acs.inorgchem.3c02569
Inorg. Chem. XXXX, XXX, XXX−XXX

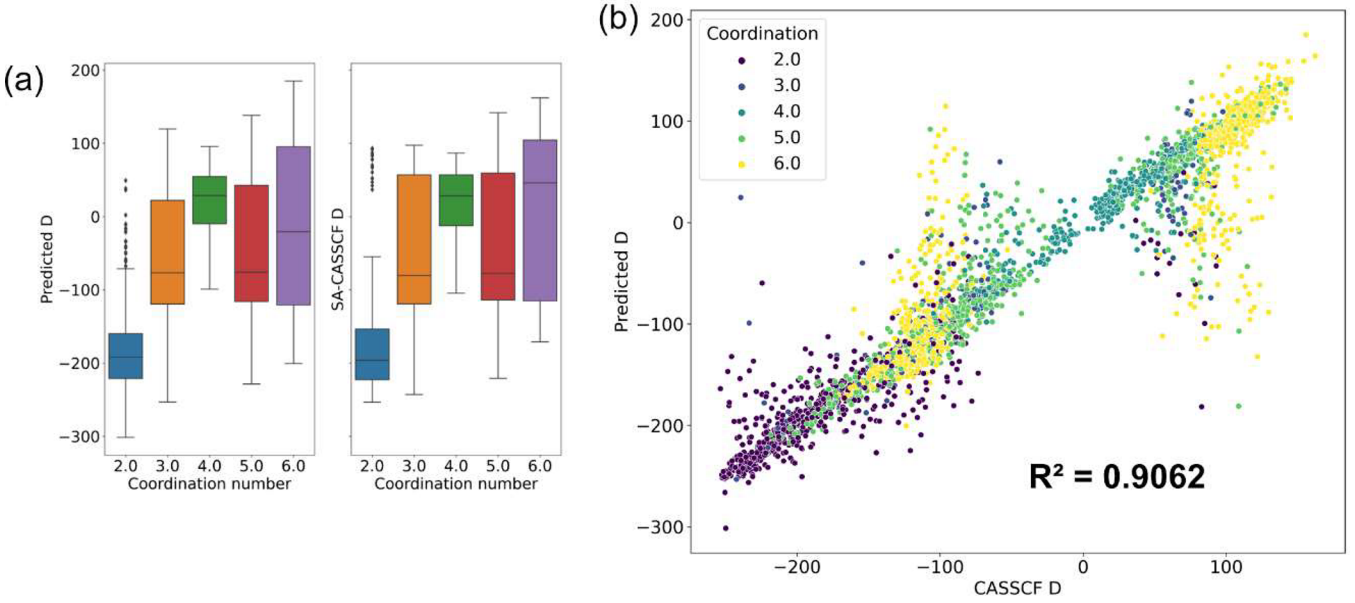

Figure 3. (a) Box plots for references and predictions. (b) Scatter plot for references (x axis) and predictions (y axis).

where λ = 1.0507 and α = 1.6733.

After each iteration, the performance of the NN was evaluated using the mean-square error (MSE; eq S2) as the loss function, and the result was weighted using the root-mean-square error (RMSE; eq S3), MAE (eq S4), and R^2 (eq S5) score. The training proceeded with asymptotic convergence for both the training and validation sets (Figure S4).

The NN achieved an RMSE of 34.51 cm^{-1} and an MAE of 18.14 cm^{-1} with R^2 = 0.9062 (Figure 3b), greatly improving the MAE of 117.70 cm^{-1} obtained by DFT. After training, the average prediction time takes approximately 50 ms (0.05 s), a duration that is 7700 times faster than a single D_{DFT} run on our HPC cluster using 16 threads for a six-coordinate molecule. Figure 3 shows that, even starting from single-reference DFT parameters, the DNN was able to reasonably extrapolate the axial anisotropic parameters compared to the reference SA-CASSCF values (see Table 1 for a sample of 10 randomly selected CAS D vs predictions and Table S1 for a 250 sample).

A thorough statistical analysis of each coordination number, condensed in the box plots of Figure 3a, clearly shows that the predicted values were efficient in reproducing the SA-CASSCF anisotropic components for high coordination numbers (from 4 to 6), replicating the same interquartile and maximum−minimum ranges as well. For low coordination numbers, however, small discrepancies are perceptible. The three-coordinate predictions present a more compressed quartile distribution, and the two-coordinate predictions show a more sparsely distributed number of outliers. The underrepresentation of two- and three-coordinate systems in our database, appearing in only 20% and 5%, respectively, of the total data set, likely contributed to penalizing the overall RMSE and MAE, including spreading to different signs predicted and visualized in Figure 3b.

In a future training iteration, with a more balanced data set that includes a higher proportion of low-coordinate molecules, we anticipate the potential for further improvement of the model, lowering the RMSE and MAE. This underrepresentation of molecules with low coordination numbers serves as a reminder of the importance of comprehensive and balanced training data in ML applications.

Although not central to our study, we tested the NN on a subset of five more intricate molecules, each with larger organic ligands unfamiliar to the DNN. These ligands, containing carbon, were chosen to keep the 2+ system. Structures **2** and **4** were obtained from the Cambridge Crystallographic Data Centre (ids: NIRTUG and BEMZIF), while **1**, **3**, and **5** were modeled from scratch. All underwent similar optimizations, with their relaxed geometries available in Lists S2−S6. This subset was added for completeness, and findings for them should be interpreted cautiously. Notably, the DNN correctly matched the signal and magnitude for four out of the five examples (Figure 4). This suggests that simpler ligands might

Table 1. Randomly Selected Samples of D (cm^{-1}) Values with Coordination Numbers, References, and Predicted Values

no.	coordination number	CAS D	predicted D
1657	3	63.86	53.83
1298	6	−107.20	−122.47
2416	3	−106.47	−118.31
1650	5	−89.46	−114.82
2552	2	36.72	2.04
2912	2	−228.83	−199.26
2664	6	−138.63	−150.02
238	4	−82.23	−97.74
1242	2	−134.33	−33.36
1641	3	−206.93	−195.81

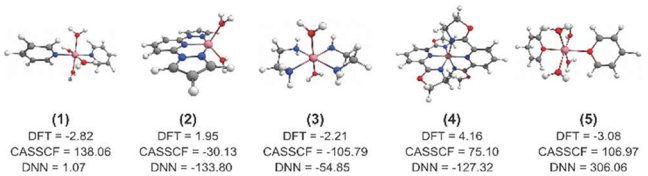

Figure 4. Unfamiliar structures comparing DFT and CASSCF D values to the NN prediction. Structures use the CPK color scheme.

https://doi.org/10.1021/acs.inorgchem.3c02569
Inorg. Chem. XXXX, XXX, XXX−XXX

simulate the field from complex ones, with the magnetic ion reacting as proposed by Griffith and Figgis.[17,36] As seen, ligands of greater denticity posed challenges, unsurprisingly given the DNN's familiarity with solely monodentate ligands. However, its good predictions hint at a promising future. As the UFF1 data set increases, accommodating varied ligands and metal centers, the NN should be capable of accurately predicting the anisotropic component, even for molecules that differ significantly from the training set.

In conclusion, our study proves that DFT data can satisfactorily predict the axial magnetic anisotropy (D) in cobalt(II) complexes. The DNN, using nine features from our UFF1 database, mirrored CASSCF D values with R^2 of 0.9062, RMSE of 34.51 cm^{-1}, and MAE of 18.14 cm^{-1}. Impressively, our method is 7700 times faster than typical D_{DFT} calculations. This approach might be extended to other magnetic centers. We also predicted axial anisotropy for four out of five unfamiliar compounds, hinting that wider training could forecast anisotropy in untrained molecules. While promising, refining hyperparameters and expanding training data can enhance accuracy. Our work highlights the ML's potential in magnetic anisotropy prediction, opening avenues for future research.

■ ASSOCIATED CONTENT

Supporting Information

The Supporting Information is available free of charge at https://pubs.acs.org/doi/10.1021/acs.inorgchem.3c02569.

Supplementary files, DFT and CASSCF detailed protocol, data preprocessing, ML protocol, Lists S1−S6, Figures S1−S4, and Tables S1 and S2 (PDF)

■ AUTHOR INFORMATION

Corresponding Authors

Glaucio B. Ferreira − *Instituto de Química, Universidade Federal Fluminense, Niterói, Rio de Janeiro 24020-141, Brazil*; Email: glauciobf@id.uff.br

Guilherme P. Guedes − *Instituto de Química, Universidade Federal Fluminense, Niterói, Rio de Janeiro 24020-141, Brazil*; orcid.org/0000-0001-6138-9943; Email: guilherme_guedes@id.uff.br

Authors

Henrique C. Silva Junior − *Instituto de Química, Universidade Federal Fluminense, Niterói, Rio de Janeiro 24020-141, Brazil*; orcid.org/0000-0003-1453-7274

Heloisa N. S. Menezes − *Instituto de Química, Universidade Federal Fluminense, Niterói, Rio de Janeiro 24020-141, Brazil*

Complete contact information is available at: https://pubs.acs.org/10.1021/acs.inorgchem.3c02569

Author Contributions

H.C.S.J., H.N.S.M., G.B.F., and G.P.G. contributed equally to this work.

Funding

This work was financially supported by the Brazilian agencies Fundação Carlos Chagas de Amparo à Pesquisa do Estado do Rio de Janeiro (Projects E-26/202.720/2018, E-26/201.314/2022, E-26/211.091/2019, E-26/010.000978/2019, E-26/010.002227/2019, and E-26/010.001801/2019), Conselho Nacional de Desenvolvimento Científico e Tecnológico (CNPq; Projects 446186/2014-7, 423086/2018-9, and 304671/2020-7), and Coordenação de Aperfeiçoamento de Pessoal de Nivel Superior Brasil within the CAPES-PrInt program, financial code 001 (Project 88887.310269/2018-00).

Notes

The authors declare no competing financial interest.

■ ACKNOWLEDGMENTS

All DFT and CASSCF calculations were performed using the Lobo Carneiro supercomputer from Núcleo Avançado de Computação de Alto Desemprenho, under Project a20006, at Laboratório Multiusuário de Química Computacional UFF and the National Laboratory for Scientific Computing (Brazil) using HPC resources of the SDumont (http://sdumont.lncc.br) supercomputer, which have contributed to the research results reported in this paper. H.N.S.M. is thankful for financial support by CNPq (PIBIC Scholarship).

■ REFERENCES

(1) Sessoli, R.; Gatteschi, D.; Caneschi, A.; Novak, M. A. Magnetic Bistability in a Metal-Ion Cluster. *Nature* **1993**, *365* (6442), 141−143.

(2) Caneschi, A.; Gatteschi, D.; Sessoli, R.; Barra, A. L.; Brunel, L. C.; Guillot, M. Alternating Current Susceptibility, High Field Magnetization, and Millimeter Band EPR Evidence for a Ground S = 10 State in [Mn12O12(Ch3COO)16(H2O)-4].2CH3COOH.4H2O. *J. Am. Chem. Soc.* **1991**, *113* (15), 5873−5874.

(3) Moneo-Corcuera, A.; Nieto-Castro, D.; Cirera, J.; Gómez, V.; Sanjosé-Orduna, J.; Casadevall, C.; Molnár, G.; Bousseksou, A.; Parella, T.; Martínez-Agudo, J. M.; Lloret-Fillol, J.; Pérez-Temprano, M. H.; Ruiz, E.; Galán-Mascarós, J. R. Molecular Memory near Room Temperature in an Iron Polyanionic Complex. *Chem.* **2023**, *9* (2), 377−393.

(4) Moreno-Pineda, E.; Wernsdorfer, W. Single-Molecule Magnets Spin Devices. *Photonic Quantum Technologies*; John Wiley & Sons, Ltd., 2023; pp 269−304. DOI: 10.1002/9783527837427.ch12.

(5) Waldmann, O. A Criterion for the Anisotropy Barrier in Single-Molecule Magnets. *Inorg. Chem.* **2007**, *46* (24), 10035−10037.

(6) Escalera-Moreno, L.; Baldoví, J. J.; Gaita-Ariño, A.; Coronado, E. Exploring the High-Temperature Frontier in Molecular Nanomagnets: From Lanthanides to Actinides. *Inorg. Chem.* **2019**, *58* (18), 11883−11892.

(7) Borah, A.; Murugavel, R. Magnetic Relaxation in Single-Ion Magnets Formed by Less-Studied Lanthanide Ions Ce(III), Nd(III), Gd(III), Ho(III), Tm(II/III) and Yb(III). *Coord. Chem. Rev.* **2022**, *453*, No. 214288.

(8) Woodruff, D. N.; Winpenny, R. E. P.; Layfield, R. A. Lanthanide Single-Molecule Magnets. *Chem. Rev.* **2013**, *113* (7), 5110−5148.

(9) Marriott, K. E. R. R.; Bhaskaran, L.; Wilson, C.; Medarde, M.; Ochsenbein, S. T.; Hill, S.; Murrie, M. Pushing the Limits of Magnetic Anisotropy in Trigonal Bipyramidal Ni(II). *Chemical Science* **2015**, *6* (12), 6823−6828.

(10) Rechkemmer, Y.; Breitgoff, F. D.; Van Der Meer, M.; Atanasov, M.; Hakl, M.; Orlita, M.; Neugebauer, P.; Neese, F.; Sarkar, B.; Van Slageren, J. A Four-Coordinate Cobalt(II) Single-Ion Magnet with Coercivity and a Very High Energy Barrier. *Nat. Commun.* **2016**, *7* (Ii), 10467.

(11) Sarkar, A.; Dey, S.; Rajaraman, G. Role of Coordination Number and Geometry in Controlling the Magnetic Anisotropy in FeII, CoII, and NiII Single-Ion Magnets. *Chem. Eur. J.* **2020**, *26* (62), 14036−14058.

(12) Soares, I. C.; Junior, H. C. S.; de Almeida, P. S. V. B.; Alves, O. C.; Soriano, S.; Ferreira, G. B.; Guedes, G. P. Coordination Polymers Containing a Pyrazole-Based Ligand and 4,4′-Bipyridine as a Spacer: Enhancing the Family of Nonzero-Dimensional Compounds Featuring Single-Ion Magnetic Behavior. *Inorg. Chem. Commun.* **2020**, *121*, No. 108201.

(13) Kumar Sahu, P.; Kharel, R.; Shome, S.; Goswami, S.; Konar, S. Understanding the Unceasing Evolution of Co(II) Based Single-Ion Magnets. *Coord. Chem. Rev.* **2023**, *475*, No. 214871.
(14) Frost, J. M.; Harriman, K. L. M. M.; Murugesu, M. The Rise of 3-d Single-Ion Magnets in Molecular Magnetism: Towards Materials from Molecules? *Chemical Science* **2016**, *7* (4), 2470−2491.
(15) Kubica, A.; Kowalewski, J.; Kruk, D.; Odelius, M. Zero-Field Splitting in Nickel(II) Complexes: A Comparison of DFT and Multi-Configurational Wavefunction Calculations. *J. Chem. Phys.* **2013**, *138* (6), No. 064304.
(16) Ferbinteanu, M.; Stroppa, A.; Scarrozza, M.; Humelnicu, I.; Maftei, D.; Frecus, B.; Cimpoesu, F. On The Density Functional Theory Treatment of Lanthanide Coordination Compounds: A Comparative Study in a Series of Cu−Ln (Ln = Gd, Tb, Lu) Binuclear Complexes. *Inorg. Chem.* **2017**, *56* (16), 9474−9485.
(17) Griffith, J. S. *The Theory of Transition-Metal Ions*; Cambridge University Press, 1964.
(18) Goodfellow, I.; Bengio, Y.; Courville, A. *Deep Learning: Adaptive Computation and Machine Learning*; MIT Press: Cambridge, MA, 2016.
(19) Lunghi, A.; Sanvito, S. Computational Design of Magnetic Molecules and Their Environment Using Quantum Chemistry, Machine Learning and Multiscale Simulations. *Nat. Rev. Chem.* **2022**, *6* (11), 761−781.
(20) Elton, D. C.; Boukouvalas, Z.; Butrico, M. S.; Fuge, M. D.; Chung, P. W. Applying Machine Learning Techniques to Predict the Properties of Energetic Materials. *Sci. Rep.* **2018**, *8* (1), 9059.
(21) Dou, B.; Zhu, Z.; Merkurjev, E.; Ke, L.; Chen, L.; Jiang, J.; Zhu, Y.; Liu, J.; Zhang, B.; Wei, G.-W. Machine Learning Methods for Small Data Challenges in Molecular Science. *Chem. Rev.* **2023**, *123*, 8736.
(22) Lunghi, A.; Sanvito, S. A Unified Picture of the Covalent Bond within Quantum-Accurate Force Fields: From Organic Molecules to Metallic Complexes' Reactivity. *Science Advances* **2019**, *5* (5), No. eaaw2210.
(23) Yu, H.; Xu, C.; Li, X.; Lou, F.; Bellaiche, L.; Hu, Z.; Gong, X.; Xiang, H. Complex Spin Hamiltonian Represented by an Artificial Neural Network. *Phys. Rev. B* **2022**, *105* (17), No. 174422.
(24) Carleo, G.; Troyer, M. Solving the Quantum Many-Body Problem with Artificial Neural Networks. *Science* **2017**, *355* (6325), 602−606.
(25) Nguyen, V. H. A.; Lunghi, A. Predicting Tensorial Molecular Properties with Equivariant Machine Learning Models. *Phys. Rev. B* **2022**, *105* (16), No. 165131.
(26) Lunghi, A.; Sanvito, S. Surfing Multiple Conformation-Property Landscapes via Machine Learning: Designing Single-Ion Magnetic Anisotropy. *J. Phys. Chem. C* **2020**, *124* (10), 5802−5806.
(27) Zaverkin, V.; Netz, J.; Zills, F.; Köhn, A.; Kästner, J. Thermally Averaged Magnetic Anisotropy Tensors via Machine Learning Based on Gaussian Moments. *J. Chem. Theory Comput.* **2022**, *18* (1), 1−12.
(28) Novikov, I.; Grabowski, B.; Körmann, F.; Shapeev, A. Magnetic Moment Tensor Potentials for Collinear Spin-Polarized Materials Reproduce Different Magnetic States of Bcc Fe. *npj Comput. Mater.* **2022**, *8* (1), 1−6.
(29) Neese, F. Software Update: The ORCA Program System, Version 4.0. *WIREs Computational Molecular Science* **2018**, *8* (1), e1327.
(30) Grimme, S.; Brandenburg, J. G.; Bannwarth, C.; Hansen, A. Consistent Structures and Interactions by Density Functional Theory with Small Atomic Orbital Basis Sets. *J. Chem. Phys.* **2015**, *143* (5), No. 054107.
(31) Neese, F. Importance of Direct Spin−Spin Coupling and Spin-Flip Excitations for the Zero-Field Splittings of Transition Metal Complexes: A Case Study. *J. Am. Chem. Soc.* **2006**, *128* (31), 10213−10222.
(32) Orio, M.; Pantazis, D. A.; Neese, F. Density Functional Theory. *Photosynth Res.* **2009**, *102* (2−3), 443−453.
(33) Yao, X.-N.; Du, J.-Z.; Zhang, Y.-Q.; Leng, X.-B.; Yang, M.-W.; Jiang, S.-D.; Wang, Z.-X.; Ouyang, Z.-W.; Deng, L.; Wang, B.-W.; Gao, S. Two-Coordinate Co(II) Imido Complexes as Outstanding Single-Molecule Magnets. *J. Am. Chem. Soc.* **2017**, *139* (1), 373−380.
(34) Díaz-Torres, R.; Menelaou, M.; Roubeau, O.; Sorrenti, A.; Brandariz-De-Pedro, G.; Sañudo, E. C.; Teat, S. J.; Fraxedas, J.; Ruiz, E.; Aliaga-Alcalde, N. Multiscale Study of Mononuclear CoII SMMs Based on Curcuminoid Ligands. *Chemical Science* **2016**, *7* (4), 2793−2803.
(35) Kaupp, M. The Role of Radial Nodes of Atomic Orbitals for Chemical Bonding and the Periodic Table. *J. Comput. Chem.* **2007**, *28* (1), 320−325.
(36) Figgis, B. N.; Hitchman, M. A. In *Ligand Field Theory and Its Applications*; King, R. B., Ed.; Wiley-VCH, 2001.
(37) Abadi, M.; Agarwal, A.; Barham, P.; Brevdo, E.; Chen, Z.; Citro, C.; Corrado, G. S.; Davis, A.; Dean, J.; Devin, M.; Ghemawat, S.; Goodfellow, I.; Harp, A.; Irving, G.; Isard, M.; Jia, Y.; Jozefowicz, R.; Kaiser, L.; Kudlur, M.; Levenberg, J.; Mane, D.; Monga, R.; Moore, S.; Murray, D.; Olah, C.; Schuster, M.; Shlens, J.; Steiner, B.; Sutskever, I.; Talwar, K.; Tucker, P.; Vanhoucke, V.; Vasudevan, V.; Viegas, F.; Vinyals, O.; Warden, P.; Wattenberg, M.; Wicke, M.; Yu, Y.; Zheng, X. TensorFlow: Large-Scale Machine Learning on Heterogeneous Distributed Systems; *arXiv* **2016**. DOI: 10.48550/arXiv.1603.04467.
(38) Bisong, E. Google Colaboratory. In *Building Machine Learning and Deep Learning Models on Google Cloud Platform*; Apress, 2019; pp 59−64. DOI: 10.1007/978-1-4842-4470-8_7.
(39) Klambauer, G.; Unterthiner, T.; Mayr, A.; Hochreiter, S. Self-Normalizing Neural Networks. *arXiv* **2017**. DOI: 10.48550/arXiv.1706.02515.
(40) Kingma, D. P.; Ba, J. Adam: A Method for Stochastic Optimization. *arXiv* **2017**. DOI: 10.48550/arXiv.1412.6980.

https://doi.org/10.1021/acs.inorgchem.3c02569
Inorg. Chem. XXXX, XXX, XXX−XXX